1 **Perpetual bioplastic production by a cyanobacteria-dominated microbiome**

2 Beatriz Altamira-Algarra[1], Artai Lage[1], Ana Lucía Meléndez[1], Marc Arnau[2,3], Eva
3 Gonzalez-Flo[1], Joan García[4]

[1] GEMMA-Group of Environmental Engineering and Microbiology. Department of Civil and Environmental Engineering. Escola d'Enginyeria de Barcelona Est (EEBE). Universitat Politècnica de Catalunya-BarcelonaTech. Av. Eduard Maristany 16. Building C5.1. E-08019 Barcelona. Spain

[2] IMEM-Innovation in Materials and Molecular Engineering. Departament d'Enginyeria Química, EEBE, Universitat Politècnica de Catalunya, C/Eduard Maristany 10-14, Barcelona, Spain

[3] Barcelona Research Center in Multiscale Science and Engineering, EEBE, Universitat Politècnica de Catalunya, C/Eduard Maristany 10-14, Barcelona, Spain

[4] GEMMA-Group of Environmental Engineering and Microbiology. Department of Civil and Environmental Engineering. Universitat Politècnica de Catalunya-BarcelonaTech. c/ Jordi Girona 1-3. Building D1. E-08034 Barcelona. Spain

* Corresponding author: joan.garcia@upc.edu

4

Abstract

Departing from the conventional axenic and heterotrophic cultures, our research ventures into unexplored territory by investigating the potential of photosynthetic microbiomes for polyhydroxybutyrate (PHB) production. A cyanobacteria-rich microbiome was harnessed for PHB production in a 3 L photobioreactor under non-sterile conditions. The robust culture achieved up to 28 $\%_{dcw}$ PHB over 108 days of alternating growth and accumulation phases. Nile Blue staining and Transmission Electron Microscope visualization successfully confirmed the presence of PHB granules within cyanobacteria cells. Analysis through proton Nuclear Magnetic Resonance further validated the extracted polymer as PHB. In addition, the overexpression of the enzyme PHA synthase throughout the accumulation phase correlated directly with the increased PHB production. Also, gene expression changes suggested that initially, glycogen served as the primary storage compound. However, with prolonged macronutrient stress, there was a shift of the carbon flux towards favoring PHB synthesis. Overall, it was demonstrated for the first time the feasibility of using a phototrophic microbiome to continuous production of PHB in a non-sterile system, contributing to advancing in the field of biopolymer production and offering valuable insights into the metabolic pathways involved.

Introduction

Environmental biotechnologies involving cyanobacteria for bioproduct generation still today face enormous scientific challenges. While numerous research have repeatedly highlighted cyanobacteria's exceptional potential for bioproducts[1–3], full-scale applications beyond the food industry remain limited. Bridging research gaps related to cyanobacterial cultures and their culture conditions is crucial to unlocking their full potential.

Among the several bioproducts synthetized by cyanobacteria, polyhydroxyalkanoates (PHA) stand out as particularly intriguing as a source for environmentally friendly non-petrochemical-based plastics[4]. Cyanobacteria can accumulate polyhydroxybutyrate (PHB, a type of PHA) under nutrient-limited conditions[2,5–8]. Nevertheless, the productivity achieved up to now by cyanobacteria wild-type (wt) strains monocultures in autotrophic conditions is not very high, being usually lower than 15 % dry cell weight (dcw) PHB. In some cases, remarkably high values of up to 20-25 $\%_{dcw}$ PHB have been reported in wild-type (wt) strains[6,9]. To enhance productivity, molecular biology techniques as introducing, overexpressing or deleting genes involved in PHB metabolism have been used[10]. However, to make PHB production processes a reality in an industrial context and cost-competitive with the current plastic market, the use of engineered strains seems not to be the most suitable strategy. An alternative procedure involves supplementing cultures with an external organic carbon source, like acetate (Ac). This has led to PHB production of up to 46 $\%_{dcw}$ PHB by cyanobacteria monocultures of *Anabaena* sp.[11], 26 $\%_{dcw}$ PHB by *Synechoccocus* sp.[6] and 22 $\%_{dcw}$ PHB by *Synechocystis* sp.[12]

Nevertheless, monocultures require precise control and sterile conditions, driving up production costs. An option could be the use of microbiomes (or mixed cultures), which in principle could have more stability than single strain cultures when growing in complex media. Microbiomes are potentially more resilient to fluctuations in environmental conditions and less susceptible to contamination with competing microorganisms. Probably, the most well-known microbiome for environmental applications is activated sludge. Studies with these organisms under heterotrophic conditions report up to 60 $\%_{dcw}$ PHB[13,14]. Nevertheless, to the authors' knowledge, the use of photosynthetic microbiomes enriched with cyanobacteria for PHB production has only been tested in very few studies, including[5,15–17].

A crucial research gap that needs to be addressed in cyanobacterial biotechnology is how to maintain productive cultures for the long-term bioproducts generation. Unfortunately, most experiments to date have been limited to short time, typically lasting only a few weeks and small-scale batch experiments under sterile conditions[8,10,18]. There have been no attempts to maintain cultures in the long term (at least for several months) for continuous bioproduct generation.

In a previous study, we assessed the viability of augmenting PHB production by enhancing the population of biopolymer-producing organisms via a dual-phase approach involving alternating cell growth on PHB and subsequent biopolymer accumulation induced by Ac addition in a dark environment[17]. Although up to 22 $\%_{dcw}$ PHB was obtained after 179 days of operation, the presence of competing green algae resulted in the destabilization of the microbiome and ultimately led to the green algae outcompeting the biopolymer-producing organisms, thus hampering PHB production stability.

In light of the above, in the present study we demonstrated for the first time the capacity of a photosynthetic microbiome enriched in cyanobacteria (and without green algae) to produce PHB over a sufficient extended period to prove perpetual production. To achieve this, we cultivated a microbiome in a photobioreactor for a total of 129 days, alternating growth/accumulation phases in controlled but non-sterile conditions. Nile Blue A staining and Transmission Electron Microscopy (TEM) were used to visualize intracellular PHB granules. We also analyzed gene expression by quantitative real-time PCR (RT-qPCR) to explore the metabolic pathways involved in PHB synthesis. Finally, the extracted polymer characterization was performed by means of Raman Spectroscopy, Fourier Transform Infrared Spectroscopy (FTIR) and proton Nuclear Magnetic Resonance (^{1}H-NMR).

The results of this study shed light on the long-term capabilities of cyanobacterial microbiomes to generate PHB, which could have significant implications for the bioplastics industry.

Results

Consistent growth and PHB accumulation by microbiome R3

We started the study by inoculating two photobioreactors (PBRs) with 100 mg volatile suspended solids (VSS)·L^{-1} of microbiome R3 obtained in[16]. The study began with the

growth phase of the conditioning cycle (Supplementary Fig. 1). A steady-state was reached at the fourth day, when the biomass (as VSS) was approximately 800 mgVSS·L^{-1} (Fig. 1). The average specific growth rate was 0.52 d^{-1} (Table 1), higher than that obtained with monocultures of *Synechocystis* sp. under similar culture conditions[6,19]. However, it took 18 days for N to be completely depleted (Supplementary Fig. 2); likely due to P limitation since it was maintained at a relatively low value (0.1 mgP·L^{-1}) to favour cyanobacteria and avoid green microalgae growth. At this point, the accumulation phase started by adding 600 mgAc·L^{-1} to the medium and enclosing the PBRs with opaque PVC tubes. Starvation phase was maintained 14 days to follow the time course of PHB synthesis by this microbiome. Biomass concentration remained constant during this phase (Fig. 1). Interestingly, biomass synthetized 11 %$_{dcw}$ PHB during the growth phase, although the conditions were not ideal for biopolymer accumulation due to nutrient presence. Nevertheless, previous studies[18] have reported significant PHB synthase activity, the enzyme involved in biopolymer synthesis, in growing cells of *Synechocystis* sp. PCC6803, the same cyanobacteria strain identified in the microbiome under investigation[16].

Biopolymer accumulation increased from 11 %$_{dcw}$ to 27 %$_{dcw}$ in seven days, when it reached the maximum. After that, PHB production slowly decreased, since at day 14 (end of the accumulation phase) PHB content was 21 %$_{dcw}$ (Fig. 1). During this period, biomass consumed 470 mgAc·L^{-1} from the 600 mgAc·L^{-1} added (Supplementary Fig. 2).

After 14 days in accumulation phase, a biomass purge was done and replaced with fresh BG-11 medium to start a new cycle (repetition 1) (Supplementary Fig. 1). Subsequent growth phases (repetition 1, 2 and 3) aimed to select PHB-producers because we assumed that the cyanobacteria will use mostly the stored PHB as carbon source since no substrate (as carbon source) was added to the medium (only the CO_2 from the injections to maintain pH, Supplementary Fig. 3).

To shorten the growth phase, we used a lower N concentration (25 mg·L^{-1}) during the repetitions' growth phase. This adjustment did not hinder the biomass growth. In fact, biomass reached an average of almost 800 mgVSS·L^{-1} in seven days (Fig. 1 and Supplementary Fig. 2), sufficient for the accumulation step[17]. Biomass exhibited an average growth rate of 0.17 d^{-1} (Table 1) in repetitions 1-3, three times slower than in the first growth performed in the conditioning cycle (μ = 0.52 d^{-1}). This difference can be attributed to a lower initial biomass concentration (100 mgVSS·L^{-1} vs. 400 mgVSS·L^{-1}),

combined with the presence of external IC (as bicarbonate), as well as higher N concentration (50 $mg \cdot L^{-1}$ vs 25 $mg \cdot L^{-1}$) in the conditioning cycle. PHB concentration declined from the beginning to the end of each growth phase, indicating that cells used the stored PHB as carbon source. Growth rate on PHB seems to be slower than that on soluble IC because growth rate on biopolymer is determined by the PHB hydrolysis rate, which is a slow process[17,20].

Regarding to PHB production, both PBRs followed a similar trend (Fig. 1). Intracellular PHB increased after Ac supplementation and 14 days in dark, peaking at day 4 of the accumulation phase, when the average was 28 $\%_{dcw}$ PHB across repetitions 1, 2 and 3 (Fig. 1). This corresponds to an average volumetric productivity of approximately 16 $mgPHB \cdot L^{-1} \cdot d^{-1}$ (Table 1). Afterward, PHB content decreased but remained relatively constant (around 24 $\%_{dcw}$ PHB) for the remainder of the accumulation phase (Fig. 1).

pH is useful to track biomass activity. During the growth phase of the conditioning period (initially adding 100 $mgIC \cdot L^{-1}$ as bicarbonate), pH fluctuations were anticipated due to photosynthesis and cell respiration, resulting in daytime rises and nighttime drops in pH (Supplementary Fig. 3). Once the pH reached the setpoint (8.5), CO_2 was injected in the PBRs to maintain it in the desired range (Supplementary Fig. 3). While 100 $mgIC \cdot L^{-1}$ were present at the start of the conditioning cycle, during repetitions 1-3 bicarbonate was not added. The available IC in the conditioning period enabled more cell grow and; therefore, the increase in pH was faster, resulting in more CO_2 supplied due to pH control (Supplementary Fig. 3). Slower increases in pH during repetitions 1-3 could be attributed to PHB consumption during those growth phases. It is difficult to compare pH trends obtained with those from heterotrophic cultures, since often pH is monitored and controlled[6,19,21,22] but pH profiles from the growth phase (referred to as the "famine phase" in heterotrophic cultures) are rarely available.

Presence of green algae overshadowed PHB production

The same methodology described above was applied to two PBRs inoculated with UP, a microbiome rich in cyanobacteria *Synechococcus* sp. and green algae (Supplementary Fig. 4C and D)[16]. In the conditioning cycle, N (50 $mgN \cdot L^{-1}$) was completely consumed in 25 days (Supplementary Fig. 5), resulting in approximately 550 $mgVSS \cdot L^{-1}$ biomass concentration (Supplementary Fig. 6) and an average specific growth rate of 0.07 d^{-1} (Supplementary Table 1). This rate was relatively lower compared to that obtained with

the microbiome R3, richer in cyanobacteria. Subsequent growth phases (repetitions 1, 2 and 3) were performed without adding bicarbonate to promote growth of PHB-producers. Green microalgae became noticeable and increased through the experiment, leading to a decrease in the fraction of cyanobacteria in the microbiome population (Supplementary Fig. 7 and 8).

Green microalgae have the ability to accumulate Ac as a carbon storage compound in the form of starch or triacylglycerol under N starvation[23,24] and darkness[25]. Therefore, the abundance of these microorganisms in the PBRs possibly increased because during the accumulation phase (when there was no N or light) they could store the added Ac, competing with cyanobacteria for this compound. They would then use it as carbon source during the subsequent growth phase. Additionally, green microalgae could grow using the remaining Ac in the PBRs when changing from phase *i* to *i*+1. Around 150 $mgAc \cdot L^{-1}$ remained after 14 days in the accumulation phase of the conditioning cycle (Supplementary Fig. 5), possibly accounting for the substantial rise in green microalgae presence during repetition 1. Their proportion increased from 14 % at the end of conditioning cycle to 75 % at the end of repetition 1, and this ratio remained constant for the remainder of the test (Supplementary Fig. 8).

Regarding to PHB production, unlike microbiome R3 that reached a maximum at day 4, microbiome UP followed a very different trend. PHB increased throughout the 14-day accumulation phase, eventually reaching a maximum value of 7 and 8 $\%_{dcw}$ PHB (3 and 4 $mgPHB \cdot L^{-1} \cdot d^{-1}$) by the end of the conditioning cycle and repetition 1, respectively (Supplementary Table 1 and Supplementary Fig. 5 and 6). Afterwards, PHB accumulation dropped in repetitions 2 and 3, when only 2 $\%_{dcw}$ PHB was detected at the end of these repetitions (Supplementary Fig. 6), representing less than 1 $mgPHB \cdot L^{-1} \cdot d^{-1}$ productivity (Supplementary Table 1). Differences in PHB production among microbiomes, as well as, its sudden decrease were clearly linked to microbiome composition. Microscope observations showed that after repetition 1, green algae were highly present in microbiome UP (Supplementary Fig. 7), whereas such microorganisms were almost undetected in biomass from R3 (Supplementary Fig. 9). Such findings suggested that the presence of microalgae overshadowed the potential production of PHB by the microbiome because green microalgae are non-PHB-producers[17,26,27].

Robustness of cyanobacterial microbiome enables high accumulation of PHB

Microscope observations were conducted at the end of each cycle (conditioning, repetitions 1-3) to assess microbiome composition. Outcomes of microbiome R3 showed that the population remained remarkably consistent (Supplementary Fig. 9). Notably, an average of 93 % of the microbiome comprised two cyanobacteria species, *Synechocystis* sp. and *Synechococcus* sp., indicating a robust and stable microbiome composition in relation to cyanobacteria population (Supplementary Fig. 9). Over the course of the study, both species dominated the culture, although *Synechocystis* sp. was more abundant (60 %) than *Synechococcus* sp. (30 %). In addition, presence of green algae decreased during the operation time; in fact, they were not observed in the microscope observations performed (Supplementary Fig. 9).

To verify accumulation of PHB by cyanobacteria and no other microorganisms, Nile blue A staining was performed in samples from the end of each cycle (conditioning and repetitions 1-3). PHB was detected using a fluorescence microscope. The positive staining with Nile blue A clearly demonstrated that cyanobacteria were involved in PHB accumulation (Supplementary Fig. 10).

Furthermore, the PBRs were operated for one more repetition (repetitions 4). At the end of the starvation phase, biovolume was calculated. Outcomes reveled a dominance of cyanobacteria *Synechocystis* sp. over *Synechoccocus* sp. (Supplementary Fig. 9). Green algae were not observed, suggesting the dominance of PHB accumulators after 108 days of operation under conditions favoring PHB producers.

High intracellular PHB content revealed by TEM

A subsequent cycle (repetition 4) of seven days of growth and seven days under starvation was done with one PBR to obtain images of the intracellular PHB-granules. Samples were collected at three time points: at the start (prior to Ac injection), the fourth day (when maximum biopolymer production occurred) and at end of the starvation phase to monitor its time course. These time points corresponded to days 101, 105 and 108 of the entire experiment, and are referred by those numbers in this section.

Biomass used as inoculum was also examined by TEM to observe and compare morphological changes in response to the continuous growth/starvation cycles performed. Inoculum cells, grown in BG-11 medium with 0.5 $mgP \cdot L^{-1}$, displayed a typical cyanobacterial cell organization (Supplementary Fig. 11A), with the thylakoid membranes occupying most of the cytoplasm volume. Small electron-dense glycogen

inclusions between the thylakoid layers could be seen. Some cells also presented slightly electron-dense inclusions located close to the thylakoid membranes (Supplementary Fig. 11A). These inclusions were not PHB nor polyphosphate granules since GC results revealed that inoculum had no intracellular PHB and both have different morphology and electron density after staining[28,29]. These spherical granules could be presumably carboxysomes and/or lipid bodies.

TEM images of samples taken during the accumulation phase revealed distinct electron-transparent inclusion bodies ("white") with a transparent appearance, located near the cell periphery, around the thylakoid membranes. These were attributed to PHB-granules (Fig. 5 and Supplementary Fig. 11B). At the phase's onset (before adding Ac, day 101), cells already contained PHB granules because they had experienced 4 cycles of growth/starvation (conditioning + repetitions 1-3), and not all PHB was consumed during the growth phases (Fig. 1 and Supplementary Fig. 11B). In fact, PHB quantifications showed that 15 $\%_{dcw}$ still remained in the biomass (Fig. 2A). Notably, at *Synechocystis* sp. cells exhibited no more than 3 PHB granules at day 101, increasing on day 105 and 108 (Fig. 2B). Indeed, the highest PHB accumulation was observed on day 105 (four days after Ac supplementation) (24 $\%_{dcw}$ PHB), with *Synechocystis* sp. presenting a maximum of 6 granules per cell, while *Synechococcus* sp. cells had up to 15 granules (Fig. 2B and C). On day 108, after 7 days in starvation, no differences were detected in the size and number of PHB-granules per cell (Supplementary Fig. 11B) with sample from day 105. Remarkably, relatively similar PHB content was also detected on both days (24 $\%_{dcw}$ PHB on day 105 and 22 $\%_{dcw}$ PHB on day 108) (Fig. 2A). PHB-granules had spherical to oval shape in both cyanobacteria species; but the granules were larger in *Synechocystis* sp. compared to *Synechococcus* sp., with average diameters of 672 ± 83 nm and 217 ± 19 nm, respectively. The high degree of variability in both the size and number of biopolymer granules among both species, as well as within cells of the same species, resulted in heterogeneous biopolymer content in the culture (Supplementary Fig. 11B), possibly due to stochastic regulation of PHB synthesis[30].

Additionally, processing TEM images by the program ImageJ revealed that cells from samples taken on day 101, 105, and 108 exhibited an estimated biopolymer content of 28 $\%_{dcw}$, 35 $\%_{dcw}$ and 20 $\%_{dcw}$, respectively. These approximate values indicate a higher PHB content compared to the results from PHB extraction and quantification by gas

chromatography (GC), except for day 108 (15 $\%_{dcw}$, 24 $\%_{dcw}$ and 22 $\%_{dcw}$, for the respective time points).

Expression of key genes involved in PHB metabolism

RT-qPCR was performed to analyze the expression of specific genes encoding key enzymes related to the metabolism of PHB was analysed in repetition 4 of R3 at the same time points in which TEM images were taken by These are the start of the starvation phase (before Ac injection), the fourth day (when maximum biopolymer production occurred), and the end of the starvation phase, corresponding to days 101, 105, and 108 of the entire experiment. Additionally, enzymes involved in glycogen metabolism were also analysed since PHB can be synthesized from intracellular glycogen pools[5,31]. Both pathways, as well as the TCA cycle, use Acetyl-CoA, which can be synthesized from Ac, as a primary precursor. Results from day 101 served as reference to compare with outcomes from day 105 and 108 (Supplementary Fig. 12). Note that RT-qPCR targeted *Synechocystis* sp. genes, given their high conservation among species[32], and to their dominance observed in microscope observations (Supplementary Fig. 9).

On day 105 (fourth day of the accumulation), the overexpression of genes related to glycogen synthesis (*glgA*, codifying for glycogen synthase), the TCA cycle (*gltA*, codifying for citrate synthase) and PHB synthesis (*phaC*, codifying for polyhydroxyalkanoate synthase) was revealed (Fig. 3A). On day 108 (seventh day of the accumulation), genes *phaC* and *glgp1* (codifying for glycogen phosphorylase, involved in glycogen catabolism) were overexpressed (Fig. 3B). The consistent overexpression of *phaC* on the fourth and seventh days of the starvation period (days 105 and 108 respectively) aligns with the observed stable PHB content (24 $\%_{dcw}$ PHB and 22 $\%_{dcw}$ PHB, on days 105 and 108 respectively).

PHB characterization

The cyanobacteria-generated polyhydroxyalkanoate was assessed with spectroscopic techniques to make a characterization of the composition of the polymer. As reported in Fig. 4A, main Raman active modes for a reference sample of PHB (PHB-R) were observed at 840 ($\boldsymbol{\nu}_1$), 1060 ($\boldsymbol{\nu}_2$), 1300 – 1500 ($\boldsymbol{\nu}_3$), 1725 ($\boldsymbol{\nu}_4$) and 2800 – 3100 cm^{-1} ($\boldsymbol{\nu}_5$) and attributed to C–COO, C–CH_3 stretching, CH_2/CH_3 bending (symmetric and antisymmetric), C=O stretching and different C–H stretching of methyl groups, respectively[33]. Raman spectra comparison between PHB-R and the PHB biogenerated

(PHB-B) showed no differences, except from a broad shoulder at 2876 cm^{-1} attributed to impurities acquired during the extraction process (Diamond mark, Fig. 4A). FTIR outcomes (Fig. 4B) corroborated the results obtained by Raman through the observation of the main vibrational modes C–CH_3 stretching, CH_2 wagging and C=O stretching (1057, 1281 and 1724 cm^{-1}, respectively) reported for PHB[33,34]. A broad band at 3000 – 4000 cm^{-1} caused by water presence was detected for the PHB-B sample leading to a poor signal-to-noise ratio at the same region.

Nonetheless, due to significant similarities in Raman and FTIR spectra between PHB and other PHAs, such as poly(3-hydroxybutyrate-co-3-hydroxyvalerate) (PHBHV, Supplementary Fig. 13 and 14), ^{1}H-NMR analysis was deemed necessary to further confirm the sole production of PHB. Careful inspection of the PHB-B NMR spectra (Fig. 4C) enabled the peak assignation of the carbons depicted in the PHB monomer (Fig. 4D).

Discussion

Research on PHA production by bacteria is extensive, but studies involving mixed cultures with cyanobacteria are relatively limited. While results on PHB synthesis by cyanobacteria pure cultures have demonstrated their potential as biopolymer producers, current production yields may not yet meet the demands of a market predominantly dominated by petroleum-based plastics. Therefore, efforts to boost their productivity should be pursued.

Here we showcase the possibility of sustained PHB synthesis by a cyanobacteria consortium through the application of repetitive biomass growth and PHB accumulation phases. Several key factors contribute to the success of our approach. Firstly, the composition of the microbiome proves crucial for maintaining PHB synthesis over time, with cyanobacteria, the primary PHB producers, requiring dominance in the culture. This strategic control results in notable 25-28 %dcw PHB, ranking among the highest values recorded by the cyanobacteria strains present in the studied community (*Synechocystis* sp. PCC 6803 and *Synechococcus* sp. PCC 6312, Table 2). Although PHB synthesis by *Synechocystis* sp. PCC 6803 has been thoroughly investigated, there is a dearth of literature available on the performance of *Synechococcus* sp. PCC 6312, nor the use of both strains in a mixed culture. Previous studies reporting PHB synthesis usually operated with monocultures under sterile conditions and in very small volumes, rarely exceeding 150 mL (Table 2). In the only report of *Synechocystis* sp. PCC 6803 tested in higher

volumes, an engineered strain (ΔSphU) was cultivated with shrimp wastewater in a 15 L PBR22. Despite reporting high intracellular PHB content (Table 2), engineered strains are not optimal for the scale-up of the process in an environmental biotechnology perspective, since production costs will increase due to the requirement of sterile conditions or synthetic substrates.

Our study stands out by demonstrating the use of a microbiome to produce PHB in a 3 L PBR, a notable departure from the other studies done in much lower volume (Table 2). In addition, production remained consistent for an impressive 108-day period, compared to tests lasting less than 2 weeks. This extended duration of steady production attests to the robustness of the culture in accumulating the desired bioproduct. Moreover, it is worth noting that our approach also streamlines operations by utilizing the same PBR for both growth and starvation phases, rather than relying on separate PBRs for each phase, including biomass harvesting steps like centrifugation[35–38]. Here, PBRs have worked under non-sterile conditions in semi-continuous mode, with minimal manipulations, such as Ac addition at the start of each starvation phase and culture purge followed by new medium replacement every 21 days (in fact the purge is the resulting product of our process). This streamlined methodology represents a significant advantage in terms of scalability, reducing both equipment requirements and processing time, ultimately leading to cost savings and increased efficiency.

We also showed that to ensure optimal PHB production, it is imperative to prevent presence of non-PHB producers, like green microalgae, in the initial inoculum. Despite the low P concentration used to prevent their proliferation during growth phases, it became evident that the stored carbon in the form of starch or triacylglycerol and/or the residual Ac significantly contributed to their growth. This indicated that P limitation alone was insufficient to hinder the growth of green microalgae. In a previous study, up to 22 $\%_{dcw}$ PHB was obtained by a microbiome rich in cyanobacteria; nevertheless, production was marked by notable fluctuations due to the presence of green algae[17]. This underscores the critical role of culture composition in achieving stable and reliable PHB production.

Secondly, we provide compelling evidence that cyanobacteria actively accumulate the biopolymer, substantiated by both Nile blue A staining and TEM images. In addition, Nile blue A staining could be used as a rapid and effective methodology to asses PHB synthesis in microbial cultures, aligning with previous reports in sludge from wastewater treatment plants[22,39–41] or the cyanobacteria *Nostoc* sp.[7]. Interestingly, TEM images

depicting cyanobacteria cultures with intracellular PHB are not commonly reported. In fact, only a few studies have described the granule size, number or intracellular content in these microorganisms (Supplementary Table 2). Most published works focus on morphological changes between WT and mutant cells, where PHB production was not the main objective[29,42,43]. However, based on the available TEM images, we can conclude that the Synechocystis sp. from our studied mixed culture exhibited one of the highest intracellular biopolymer contents, as well as the greatest number of granules (Supplementary Table 2). Much limited information is found regarding PHB production by *Synechoccocus* sp. From TEM images by[44] and the current study (Fig. 2), *Synechoccocus* sp. presented a higher number of granules, but smaller in size, compared to Synechocystis sp. (Supplementary Table 2).

Furthermore, upon processing TEM images by the ImageJ program, we observed a discrepancy between results obtained from PHB extraction from lyophilized biomass and those from image processing. This could be attributed to the larger size and heavier cyanobacterial cells in comparison to heterotrophic bacterial cells[18], leading to incomplete biopolymer extraction; a crucial step prior to GC analysis. Consequently, quantification of PHB content in cyanobacteria tends to be lower. This suggests that the studied microbiome has even greater potential for PHB accumulation, considering the variability in PHB content among cells, as and the underestimation of GC results.

Thirdly, the overexpression of gene *phaC* exhibited a direct correlation with increased PHB production during the accumulation phase. PhaC is the key enzyme in PHB synthesis. For instance, *Synechocystis* sp. lacking *phaC* (Δ*phaC*) failed to produce PHB when Ac was added to the medium[45]. In our study, a direct relation between the increase in PHB production (Fig. 2A) and the overexpression of gene *phaC* from day 101 to day 105 and 108 was evident (Fig. 3). The overexpression of this gene in the fourth and seventh day of the starvation (days 105 and 108, respectively) was similar, which agrees with the observed constant PHB content (24 $\%_{dcw}$ PHB in day 105 and 22 $\%_{dcw}$ PHB in day 108). This suggested that polymer synthesis from acetate was a relatively fast process since it reached a maximum in four days remaining constant thereafter. In addition to PHB, cyanobacteria also accumulate glycogen as carbon storage compund[5,45]. Outcomes showed that in day 105, glycogen synthesis was underway, as evidenced by the overexpression of *glgA* (Fig. 3A and Supplementary Fig. 12). This gene expression, however, decreased after three days (day 108) (Fig. 3B and Supplementary Fig. 12),

indicating that glycogen was the initial storage compound synthesized in response to short-term macronutrient stress conditions, such as nitrogen depletion, as reported by other authors[30,45–47]. Nevertheless, the higher expression of *gltA* on day 105 (Fig. 3A and Supplementary Fig. 12) indicated that part of the Acetyl-CoA was channeled into the TCA cycle instead of being used to produce PHB. Interestingly, this gene was not overexpressed on day 108, suggesting a decrease in carbon flux to TCA, possibly favoring PHB synthesis.

On day 108, cells accumulated 22% $_{dcw}$ PHB, as confirmed biopolymer extraction results, and the overexpression of *phaC* (Fig. 2A and Fig. 3B). At this time point, overexpression of genes involved in glycogen synthesis was not detected, further reinforcing the rapid synthesis of glycogen as consequence of nutrients starvation and later PHB accumulation. Additionally, glycogen degradation was active, as indicated by the overexpression of gene *glgp1* (Fig 3B and Supplementary Fig. 12). The stored glycogen was being oxidized due to N-starvation persistence, with degradation products ultimately contributing to the conversion to PHB. This would explain the sustained intracellular PHB content after 7 days in starvation by the overexpression of *phaC*, with no observed PHB decrease. These findings agreed with other studies reporting conversion of glycogen to PHB in cyanobacteria[31,46,48]. The degradation of glycogen and its transformation into PHB occurs during prolonged N-starvation to mitigate the potential osmotic impacts of excessive intracellular metabolites accumulation and to generate ATP to maintain basic cellular functions[49,50]. This result elucidated the metabolic dynamics underlying PHB synthesis.

Finally, we conducted Raman, FTIR and ^{1}H-NMR analysis to characterize the synthetized biopolymer. Results clearly showed that the biopolymer accumulated by the studied consortium was PHB. While certain cyanobacteria strains are cable of producing co-polymer PHBV[51], absence of peaks with possible attribution to other polymers was observed, providing conclusive evidence for the exclusive synthesis of PHB by *Synechocystis* sp. and *Synechococcus* sp., the cyanobacteria present in the studied microbiome. This conclusion was further supported by additional ^{1}H-NMR measurements conducted on PHB-R and PHBHV (Supplementary Fig. 15 and 16).

Methods

Inoculum and experimental set-up

Two microbiomes isolated in[16], named R3 and UP, were used as the inoculum for 3 L glass cylindrical photobioreactors (PBRs) of 2.5 L working volume (Supplementary Fig. 17). Microbiome sample R3 was collected from the Besòs River (Sant Adrià de Besòs, Spain, 41°25'20.2"N 2°13'38.2"E), an intermittent Mediterranean stream that receives high amounts of treated wastewater discharged from the sewage treatment plants in the metropolitan area of Barcelona. This microbiome was rich in the unicellular cyanobacteria *Synechocystis* sp. and *Synechococcus* sp. (Supplementary Fig. 4A and B) because of the applied selective pressure described in [16]. These organisms were identified as *Synechocystis* sp. PCC6803 and *Synechococcus* sp. PCC 6312 by phylogenetic analysis based on 16S rRNA gene sequences with the highest similarity, 100 % confidence and 97 % confidence, respectively[16]. UP sample was collected from an urban pond located in Diagonal Mar Park (Barcelona, Spain, 41°24'31.0"N 2°12'49.9"E), which is fed with groundwater water. The microbiome was rich in the cyanobacteria *Synechococcus* sp., identified as *Synechococcus* sp. PCC 6312 with 99 % confidence, and also had green algae (Supplementary Fig. 4C and D).

Illumination in reactors was kept at 30 klx (approx. 420 $\mu mol \cdot m^{-2} \cdot s^{-1}$) by 200 W LED floodlight, placed at 15 cm from the reactors surface in 15:9 h light:dark cycles (during growth phase). pH was measured online with a pH probe (HI1001, HANNA instruments, Italy) placed inside the reactors and was controlled at 8 ± 0.5 (during growth phase) by a pH controller (HI 8711, HANNA instruments, Italy). The control system activated an electrovalve which allowed to inject CO_2 inside the reactors when pH reached 8.5. The pH data was saved in a 5 min interval in a computer with the software PC400 (Campbell Scientific). In PHB-accumulation phases (see below) the pH was measured but not controlled in order to avoid IC injection. The pH always maintained in values 7.5 ± 0.5 in this phase. PBRs were enclosed in opaque PVC tubes during accumulation phase to ensure dark conditions. Reactors were continuously agitated by a magnetic stirrer ensuring a complete mixing and culture temperature was kept at 30-35 ºC. Two PBRs were used as duplicates.

Experimental strategy

Methodology described in[17] based in cycles of alternation of growth/starvation phases was applied for 108 days (Supplementary Fig. 1). Briefly, experiment started with a conditioning period consisting on a unique cycle with one growth and starvation phases. The growth phase started with the inoculation of the PBR with a biomass concentration

of 100 mg volatile suspended solids (VSS)·L^{-1}. BG-11 with modified concentrations of bicarbonate, as source of IC, N and P (100 mgIC L^{-1}, 50 mgN·L^{-1} and 0.1 mgP·L^{-1}) was used as media (Table 3). When N was depleted, the starvation phase began. 600 mg Ac·L^{-1} was added at this point and PBRs were enclosed with PVC tubes to avoid light penetration.

After this first cycle, a total of five cycles were repeated for microbiome R3, and three for UP since microbiome composition led to low PHB synthesis (Supplementary Fig. 6). At the beginning of each cycle, a volume, usually ranging from 800 mL to 1,200 mL, was discarded from the PBRs to purge the culture broth and set approximately 400 mgVSS·L^{-1} as initial biomass concentration in each cycle. Discarded volume was replaced with new BG-11 medium with 25 mgN·L^{-1}, 0.1 mgP·L^{-1} and without IC to start the growth phase. A daily dose of a solution of KH_2PO_4 was conducted to maintain a certain P concentration inside the reactors (aprox. 0.1 mgP·L^{-1}). Each growth phase lasted seven days, until N was depleted. After that, the starvation phase started with the addition of acetate to reach 600 mgAc·L^{-1} in the cultures. All the starvation phases went on for 14 days each; except in repetition 4 with microbiome R3, which only lasted a week.

Analytical methods

At selected times, 50 mL samples were taken from each PBR. Biomass concentration was determined as VSS according to procedures in[52]. Turbidity was measured with turbidimeter (HI93703, HANNA Instruments). For a quick estimation of biomass, VSS and turbidity were correlated by calibration curve (Supplementary Fig. 18).

To determine the concentration of dissolved chemical species, samples collected from the reactors were first filtered through a 0.7 µm pore glass microfiber filter. Nitrate and phosphate were quantified following Standard Methods[52]. Note that in BG-11 the only source of N is nitrate. The filtered samples were passed through a 0.45 µm pore size filter a second time to determine Ac (acetate) by ion chromatography (CS-1000, Dionex Corporation, USA).

Microscopy

Biomass composition was tracked at the end of each cycle through the use of bright light and fluorescence microscopy observations (Eclipse E200, Nikon, Japan). Cyanobacteria and green algae were identified and classified based on morphological descriptions[53,54]. Cell counting was done in a Neubauer chamber at the end of each starvation phase.

Individual cells were counted until reach >400 cells to minimize the margin error to less than 10 %[55].

Intracellular PHB in the biomass was observed by staining cells. Small aliquots of samples from the reactors were heat-fixed on glass slides and stained with 1% Nile Blue for 10 min at room temperature. Excess dye was removed with distilled water. 8% acetic acid solution was applied for 1 min at room temperature, washed with distilled water and the slide was allowed to air dry. The stained samples were examined under fluorescence microscopy at excitation and emission wavelength of 510 nm and 590 nm, respectively.

Transmission Electron Microscope

At the start of the starvation phase (prior to Ac injection), the fourth day and at the end of the starvation phase in repetition 4, 4 mL samples from the reactors were centrifuged (2,000 rpm, 10 min). The supernatant was discarded and the pellet was resuspended in fixative 2% paraformaldehyde and 2.5% glutaraldehyde in 0.1 M PB. Fixation was done at room temperature for 2 h. Then, cells were washed four times in 0.1 M PB. Fixed material was subjected to osmification for 3 h at 4 ºC. After that time, samples were washed four times with MilliQ water and stored in 0.1M PB buffer at 4 ºC. Samples were dehydrated through a graded ethanol series at 4 ºC and gentle agitation (one change of 10 min in 50 % ethanol, two changes of 10 min each in 70, 90 and 96 % ethanol and three changes of 15 min each in 100% ethanol). Samples were embedded using EPON 812 resin kit molds and left 72 h in silicon molds in an oven at 60 ºC to polymerize. Ultra-thin sections (100 nm) were cut on a SORVALL MT2-B ultramicrotome with a Diatome 45 º diamond blade, collected on Formvar-coated 300-mesh coper grids and left to dry 15 h. Finally, samples were stained with UA-zero® and 3 % lead citrate and left to dry 12 h. The sections were examined in a PHILLIPS TECNAI-10 electron microscope operated at 100 kV.

Image processing and analysis

Image analysis was performed using FIJI-ImageJ software. TEM images corresponding to different time points (day 101, 105, and 108) during the accumulation phase of repetition 4 were utilized to measure the size of PHB granules produced in each strain. Prior to measurement, the TEM images were calibrated using a scalebar and the arrow tool to obtain accurate dimensions of the PHB granules. For calculating the approximate percentage of PHB, the TEM images were first segmented to obtain two black and white

images: (i) a mask representing the cell area, and (ii) a mask containing the PHB granules. To calculate the area of (i) cells and (ii) PHB granules, image analysis was applied using the measurements tool. Subsequently, the percentage of PHB granules was computed by dividing the number of pixels in the PHB granule mask by the number of pixels in the cell area mask.

RNA extraction and quantitative real-time PCR

In repetition 4, samples were collected at the start (prior to Ac injection), the fourth day and at the end of the starvation phase. Methodology was adapted from[46]. Fresh biomass (10 mL) was harvested by centrifugation at 14,000 rpm for 5 min at 4 ºC and stored at –80 ºC in an ultra-freezer (Arctiko, Denmark). Frozen cells were homogenized in lysis buffer and TRIzol followed by Bead Beating for cell lysis. Afterward, RNA was isolated using the PureLink RNA Mini Kit (Ambion, Thermo fisher Scientific, Waltham, USA) following the manufacturer's recommendations. The purified RNA was quantified using a Take3 microvolume plate (Synergy HTX, Agilent, USA). The RNA was reverse transcribed using the RevertAidTM Kit (ThermoFisher Scientific, USA) using 100 ng of total RNA according to manufacturer's protocol with a combination of the provided oligo (dT) and random hexamer primers (20 µL). The quality and quantity of the cDNA fragments was analyzed using a Take3 microvolume plate (Synergy HTX, Agilent, USA).

Gene expression levels were determined using the qPCR thermocycler Quantstudio 3 (ThermoFisher Scientific, USA). To do this, designed primers described in[46] at 300 nM and the Powerup SYBR master mix (ThermoFisher Scientific, USA) were used. The 16S RNA was selected as the housekeeping gene as the one with lower variability between the different tested conditions. For the results, the mean Ct values were determined using the method from[56] by calculating the average of the triplicate measurements for each condition and gene. The ΔCt was calculated by subtracting the mean Ct value of the housekeeping gene from the mean Ct value of the gene of interest. ΔΔCt is the difference between ΔCt of the day 3, and 7 of accumulation and the ΔCt of day 1 (before adding Ac) as control Ct values. Finally, to calculate the relative fold gene expression level, 2 to the power of negative ΔΔCt according to equation 1:

$$\text{Fold gene expression} = 2^{-(\Delta\Delta Ct)} \quad (1)$$

Statistical analysis was performed by one-way ANOVA to evaluate the possible interaction between genes. P-values lower than 5 % were considered statistically significant.

PHB extraction and quantification

PHB analysis was done for samples collected during starvation phases for both microbiomes. Methodology was adapted from described in [57]. Concisely, 50 mL of mixed liquor were collected and centrifuged (4,200 rpm, 7.5 min), frozen at −80 °C overnight in an ultra-freezer (Arctiko, Denmark) and finally freeze-dried for 24 h in a freeze dryer (−110 ºC, 0.05 hPa) (Scanvac, Denmark). 3-3.5 mg of freeze-dried biomass were mixed with 1 mL CH_3OH with H_2SO_4 (20% v/v) and 1 mL $CHCl_3$ containing 0.05 % w/w benzoic acid. Samples were heated for 5 h at 100 ºC in a dry-heat thermo-block (Selecta, Spain). Then, they were placed in a cold-water bath for 30 min to ensure they were cooled. After that, 1 mL of deionized water was added to the tubes and they were vortexed for 1 min. $CHCl_3$ phase, containing PHB dissolved, was recovered with a glass pipette and introduced in a chromatography vial containing molecular sieves. Samples were analysed by gas chromatography (GC) (7820A, Agilent Technologies, USA) using a DB-WAX 125-7062 column (Agilent Technologies, USA). Helium was used as the gas carrier (4.5 $mL \cdot min^{-1}$). Injector had a split ratio of 5:1 and a temperature of 230 °C. FID had a temperature of 300 °C. A standard curve of the co-polymer PHB-HV was used to quantify the PHB content.

PHB characterization

Raman spectra of the samples were acquired using an inVia Qontor confocal Raman microscope (Renishaw) equipped with a Renishaw Centrus 2957T2 detector and a 785 nm laser. All the measurements were performed in mapping mode (64 points) to ensure obtention of representative data. FTIR vibrational studies were recorded on a FTIR Nicolete 6700 spectrometer through a SmartOrbit ATR accessory with Ge crystal and DTGS/CsI detector. Each sample measurement was performed between 4000 – 675 cm^{-1} with a 2 cm^{-1} resolution and spectra processing was carried out using the OMNIC Spectroscopy software. The synthesized polymer and references were analysed through ^{1}H-NMR spectroscopy; using a Bruker Avance III-400 spectrometer operating at 400.1 MHz. The chemical shift was calibrated using tetramethylsilane as internal standard and

568 the samples were dissolved in deuterated chloroform ($CDCl_3$). Recording of 256 scans
569 was performed for all samples.

570 **Calculations**

571 Total biovolumes (BV) in $mm^3 \cdot L^{-1}$ of each species (cyanobacteria (*Synechocystis* sp. and
572 *Synechococcus* sp.) and the green microalgae) were calculated using the formula:

573 $$BV = \frac{n \cdot V}{10^6} \quad (2)$$

574 where n is the number of cells counted in a sample ($cells \cdot L^{-1}$) and V is the average volume
575 of each species (μm^3). 10^6 is a factor conversion from $\mu m^3 \cdot mL^{-1}$ to $mm^3 \cdot L^{-1}$. Cell volume
576 was calculated by volumetric equations of geometric shape closest to the cells of each
577 species. Volume equations of sphere, cylinder and ellipsoid were used for BV calculation
578 of *Synechocystis* sp., *Synechococcus* sp. and green algae, respectively (Supplementary
579 Table 3). Cell dimensions (length and width) were obtained from images of microscope
580 observations (software NIS- Element viewer®).

581 Kinetic coefficients were calculated as follows:

582 Specific growth rate (d^{-1}) was calculated using the general formula

583 $$\mu_X = \frac{\ln(x)_{ti} - \ln(x)_{t0}}{t_i - t_o} \quad (3)$$

584 where $\ln(X)_{ti}$ and $\ln(X)_{tn}$ are the natural logarithms of the biomass concentration
585 ($mgVSS \cdot L^{-1}$) at experimental day (t_i) and at the beginning of the growth phase (t_0),
586 respectively. t_i values were considered as the day when biomass concentration reached
587 stationary phase).

588 Biomass volumetric production rate ($mg \cdot L^{-1} \cdot d^{-1}$) was calculated as:

589 $$r_X = \frac{X_{ti} - X_{to}}{t_i - t_0} \quad (4)$$

590 where X_{ti} ($mg \cdot L^{-1}$) and X_{t0} ($mg \cdot L^{-1}$) are the biomass concentration (in $mgVSS \cdot L^{-1}$) at time
591 t_i (when biomass reached stationary phase) and at the beginning of the growth phase (t_0).
592 *i* is the total number of days that the growth phase lasted.

593 The nitrogen (N) to biomass (X) yield was calculated only during the growth phase by:

594 $$Y_{X/N} = \frac{VSS_{ti} - VSS_{t0}}{N_{ti} - N_{t0}} \quad (5)$$

where VSS_{ti} ($mg \cdot L^{-1}$) and VSS_{t0} ($mg \cdot L^{-1}$) are the biomass concentration at the end (t_i) and at the start of the phase (t_0). N_{ti} ($mg \cdot L^{-1}$) and N_{t0} ($mg \cdot L^{-1}$) are the nitrogen concentration ($N\text{-}NO_3^-$) at the end and at the beginning of each growth phase, respectively.

The specific consumption rate of nitrogen ($mgN \cdot mgVSS^{-1} \cdot d^{-1}$) was calculated as:

$$q_{N-NO3} = \frac{\mu_X}{Y_{X/N}} \quad (6)$$

where μ_X was obtained as shown in equation 3 and $Y_{X/N}$ in equation 5.

PHB volumetric production rate (Υ_{PHB} ($mgPHB \cdot L^{-1} \cdot d^{-1}$)) was obtained by:

$$\Upsilon_{PHB} = \frac{(\%_{dcw}PHB_{ti} \cdot X_{ti} - \%_{dcw}PHB_{t0} \cdot X_{t0})/100}{t_i - t_0} \quad (7)$$

where $\%_{dcw}PHB_{ti}$ and $\%_{dcw}PHB_{t0}$ are the percentage of PHB respect biomass quantified at time *i* (end of accumulation phase) and at the beginning of the accumulation phase (t_0). X_{ti} and X_{to} are the biomass concentration (in $mgVSS \cdot L^{-1}$) at the beginning (t_0) and end of the accumulation phase (t_i).

The PHB yield on acetate (Ac) ($Y_{PHB/Ac}$) was calculated on a COD-basis by:

$$Y_{PHB/Ac} = \frac{PHB_{ti} - PHB_{t0}}{600 - Ac_{ti}} \quad (8)$$

The amount of PHB produced (given as chemical oxygen demand (COD): 1.67 $gCOD \cdot gPHB^{-1}$) was obtained by multiplying the $\%_{dcw}$ PHB produced per biomass concentration (in $mgVSS \cdot L^{-1}$) at time *i* (experimental day) and at the beginning (t_0) of the accumulation phase. Ac_{ti} ($mg \cdot L^{-1}$) is the acetate concentration (given 1.07 $gCOD \cdot gAc^{-1}$) at the experimental day (t_i) of the starvation phase. 600 $mgAc \cdot L^{-1}$ is the amount of added acetate.

References

1. Senatore, V. *et al.* Production of phycobiliproteins, bioplastics and lipids by the cyanobacteria Synechocystis sp. treating secondary effluent in a biorefinery approach. *Sci. Total Environ.* **857**, (2023).

2. Yashavanth, P. R., Das, M. & Maiti, S. K. Recent progress and challenges in cyanobacterial autotrophic production of polyhydroxybutyrate (PHB), a bioplastic. *J. Environ. Chem. Eng.* **9**, (2021).

623 3. Pagels, F., Guedes, A. C., Amaro, H. M., Kijjoa, A. & Vasconcelos, V.
624 Phycobiliproteins from cyanobacteria: Chemistry and biotechnological
625 applications. *Biotechnol. Adv.* **37**, 422–443 (2019).

626 4. Chen, G.-Q. Industrial Production of PHA. **14**, 121–132 (2010).

627 5. Rueda, E. *et al.* Polyhydroxybutyrate and glycogen production in
628 photobioreactors inoculated with wastewater borne cyanobacteria monocultures.
629 *Bioresour. Technol.* **295**, 122233 (2020).

630 6. Rueda, E., Altamira-Algarra, B. & García, J. Process optimization of the
631 polyhydroxybutyrate production in the cyanobacteria Synechocystis sp. and
632 Synechococcus sp. *Bioresour. Technol.* **356**, 127330 (2022).

633 7. Ansari, S. & Fatma, T. Cyanobacterial Polyhydroxybutyrate (PHB): Screening,
634 Optimization and Characterization. *PLoS One* **11 (6)**, (2016).

635 8. Monshupanee, T. & Incharoensakdi, A. Enhanced accumulation of glycogen,
636 lipids and polyhydroxybutyrate under optimal nutrients and light intensities in the
637 cyanobacterium Synechocystis sp. PCC 6803. *J. Appl. Microbiol.* **116**, 830–838
638 (2014).

639 9. Panda, B., Jain, P., Sharma, L. & Mallick, N. Optimization of cultural and
640 nutritional conditions for accumulation of poly-β-hydroxybutyrate in
641 Synechocystis sp. PCC 6803. *Bioresour. Technol.* **97**, 1296–1301 (2006).

642 10. Khetkorn, W., Incharoensakdi, A., Lindblad, P. & Jantaro, S. Enhancement of
643 poly-3-hydroxybutyrate production in Synechocystis sp. PCC 6803 by
644 overexpression of its native biosynthetic genes. *Bioresour. Technol.* **214**, 761–
645 768 (2016).

646 11. Simonazzi, M. *et al.* Production of polyhydroxybutyrate by the cyanobacterium
647 cf. Anabaena sp. *Int. J. Biol. Macromol.* **191**, 92–99 (2021).

648 12. Panda, B. & Mallick, N. Enhanced poly-b-hydroxybutyrate accumulation in a
649 unicellular cyanobacterium, Synechocystis sp. PCC 6803. *Lett. Appl. Microbiol.*
650 **44**, 194–198 (2007).

651 13. Estévez-Alonso, Á. *et al.* Calcium enhances polyhydroxyalkanoate production
652 and promotes selective growth of the polyhydroxyalkanoate-storing biomass in

municipal activated sludge. *Water Res.* **226**, 119259 (2022).

14. Crognale, S. *et al.* Effect of the organic loading rate on the PHA-storing microbiome in sequencing batch reactors operated with uncoupled carbon and nitrogen feeding. *Sci. Total Environ.* **825**, (2022).

15. Arias, D. M. *et al.* Polymer accumulation in mixed cyanobacterial cultures selected under the feast and famine strategy. *Algal Res.* **33**, 99–108 (2018).

16. Altamira-Algarra, B. *et al.* New strategy for bioplastic and exopolysaccharides production: Enrichment of field microbiomes with cyanobacteria. *bioRxiv* 2023.05.30.542819 (2023) doi:10.1101/2023.05.30.542819.

17. Altamira-Algarra, B., Lage, A., García, J. & Gonzalez-Flo, E. Species composition determines bioplastics production in photosynthetic microbiomes: strategy to enrich cyanobacteria PHB-producers. *bioRxiv* 2023.05.30.542808 (2023) doi:10.1101/2023.05.30.542808.

18. Sudesh, K., Taguchi, K. & Doi, Y. Effect of increased PHA synthase activity on polyhydroxyalkanoates biosynthesis in Synechocystis sp. PCC6803. *Int. J. Biol. Macromol.* **30**, 97–104 (2002).

19. Rueda, E., Gonzalez-Flo, E., Roca, L., Carretero, J. & Garciá, J. Accumulation of polyhydroxybutyrate in Synechocystis sp. isolated from wastewaters: Effect of salinity, light, and P content in the biomass. *J. Environ. Chem. Eng.* **10**, 107952 (2022).

20. Third, K. A., Burnett, N. & Cord-Ruwisch, R. Simultaneous nitrification and denitrification using stored substrate (PHB) as the electron donor in an SBR. *Biotechnol. Bioeng.* **83**, 706–720 (2003).

21. Burniol-Figols, A. *et al.* Polyhydroxyalkanoates (PHA) production from fermented crude glycerol: Study on the conversion of 1,3-propanediol to PHA in mixed microbial consortia. *Water Res.* **128**, 255–266 (2018).

22. Carvalheira, M. *et al.* Valorization of Brewery Waste through Polyhydroxyalkanoates Production Supported by a Metabolic Specialized Microbiome. *Life* **12**, 1–14 (2022).

23. Fan, J. *et al.* Oil accumulation is controlled by carbon precursor supply for fatty

683 acid synthesis in Chlamydomonas reinhardtii. *Plant Cell Physiol.* **53**, 1380–1390
684 (2012).

685 24. Bogaert, K. A. *et al.* Metabolic, physiological, and transcriptomics analysis of
686 batch cultures of the green microalga Chlamydomonas grown on different acetate
687 concentrations. *Cells* **8**, 1–21 (2019).

688 25. Turon, V., Trably, E., Fayet, A., Fouilland, E. & Steyer, J. P. Raw dark
689 fermentation effluent to support heterotrophic microalgae growth: Microalgae
690 successfully outcompete bacteria for acetate. *Algal Res.* **12**, 119–125 (2015).

691 26. Arias, D. M., Uggetti, E., García-Galán, M. J. & García, J. Cultivation and
692 selection of cyanobacteria in a closed photobioreactor used for secondary effluent
693 and digestate treatment. *Sci. Total Environ.* **587**–**588**, 157–167 (2017).

694 27. Fradinho, J. C., Oehmen, A. & Reis, M. A. M. Effect of dark/light periods on the
695 polyhydroxyalkanoate production of a photosynthetic mixed culture. *Bioresour.*
696 *Technol.* **148**, 474–479 (2013).

697 28. Tsang, T. K., Roberson, R. W. & Vermaas, W. F. J. Polyhydroxybutyrate
698 particles in Synechocystis sp. PCC 6803: Facts and fiction. *Photosynth. Res.* **118**,
699 37–49 (2013).

700 29. Solovchenko, A. *et al.* Phosphorus Feast and Famine in Cyanobacteria: Is Luxury
701 Uptake of the Nutrient Just a Consequence of Acclimation to Its Shortage? *Cells*
702 **9**, (2020).

703 30. Koch, M., Orthwein, T., Alford, J. T. & Forchhammer, K. The Slr0058 Protein
704 From Synechocystis sp. PCC 6803 Is a Novel Regulatory Protein Involved in
705 PHB Granule Formation. *Front. Microbiol.* **11**, 1–13 (2020).

706 31. Koch, M., Doello, S., Gutekunst, K. & Forchhammer, K. PHB is produced from
707 glycogen turn-over during nitrogen starvation in Synechocystis sp. PCC 6803.
708 *Int. J. Mol. Sci.* **20**, (2019).

709 32. Hai, T., Hein, S. & Steinbüchel, A. Multiple evidence for widespread and general
710 occurrence of type-III PHA synthases in cyanobacteria and molecular
711 characterization of the PHA synthases from two thermophilic cyanobacteria:
712 Chlorogloeopsis fritschii PCC 6912 and Synechococcus sp. strain MA1.

Microbiology **147**, 3047–3060 (2001).

33. Izumi, C. M. S. & Temperini, M. L. A. FT-Raman investigation of biodegradable polymers: Poly(3-hydroxybutyrate) and poly(3-hydroxybutyrate-co-3-hydroxyvalerate). *Vib. Spectrosc.* **54**, 127–132 (2010).

34. Bayari, S. & Severcan, F. FTIR study of biodegradable biopolymers: P(3HB), P(3HB-co-4HB) and P(3HB-co-3HV). *J. Mol. Struct.* **744–747**, 529–534 (2005).

35. Mariotto, M., Egloff, S., Fritz, I. & Refardt, D. Cultivation of the PHB-producing cyanobacterium Synechococcus leopoliensis in a pilot-scale open system using nitrogen from waste streams. *Algal Res.* **70**, 103013 (2023).

36. Koch, M. *et al.* Maximizing PHB content in Synechocystis sp. PCC 6803: a new metabolic engineering strategy based on the regulator PirC. *Microb. Cell Fact.* **19**, 1–12 (2020).

37. Gracioso, L. H. *et al.* Light excess stimulates Poly-beta-hydroxybutyrate yield in a mangrove-isolated strain of Synechocystis sp. *Bioresour. Technol.* **320**, 1–7 (2021).

38. Troschl, C. *et al.* Pilot-scale production of poly-β-hydroxybutyrate with the cyanobacterium Synechocytis sp. CCALA192 in a non-sterile tubular photobioreactor. *Algal Res.* **34**, 116–125 (2018).

39. Oshiki, M. ., Satoh, H. . & Mino, T. Rapid quantification of polyhydroxyalkanoates (PHA) concentration in activated sludge with the fluorescent dye Nile blue A. *Water Sci. Technol.* **64 (3)**, 747–753 (2011).

40. Sruamsiri, D., Thayanukul, P. & Suwannasilp, B. B. In situ identification of polyhydroxyalkanoate (PHA)-accumulating microorganisms in mixed microbial cultures under feast/famine conditions. *Sci. Rep.* **10**, 1–10 (2020).

41. Mesquita, D. P. *et al.* Polyhydroxyalkanoate granules quantification in mixed microbial cultures using image analysis : Sudan Black B versus Nile Blue A staining. *Anal. Chim. Acta* **865**, 8–15 (2015).

42. Nagarajan, S., Srivastava, S. & Sherman, L. A. Essential role of the plasmid hik31 operon in regulating central metabolism in the dark in Synechocystis sp. PCC 6803. *Mol. Microbiol.* **91**, 79–97 (2014).

743 43. Klotz, A. *et al.* Awakening of a Dormant Cyanobacterium from Nitrogen
744 Chlorosis Reveals a Genetically Determined Program. *Curr. Biol.* **26**, 2862–2872
745 (2016).

746 44. Asada, Y., Miyake, M., Miyake, J., Kurane, R. & Tokiwa, Y. Photosynthetic
747 accumulation of poly-(hydroxybutyrate) by cyanobacteria - The metabolism and
748 potential for CO2 recycling. *Int. J. Biol. Macromol.* **25**, 37–42 (1999).

749 45. Damrow, R., Maldener, I. & Zilliges, Y. The multiple functions of common
750 microbial carbon polymers, glycogen and PHB, during stress responses in the
751 non-diazotrophic cyanobacterium Synechocystis sp. PCC 6803. *Front.*
752 *Microbiol.* **7**, 1–10 (2016).

753 46. Rueda, E. *et al.* Inorganic carbon stimulates the metabolic routes related to the
754 polyhydroxybutyrate production in a Synechocystis sp. strain (cyanobacteria)
755 isolated from wastewater. *Sci. Total Environ.* **829**, (2022).

756 47. Forchhammer, K. & Schwarz, R. Nitrogen chlorosis in unicellular cyanobacteria
757 – a developmental program for surviving nitrogen deprivation. *Environ.*
758 *Microbiol.* **21**, 1173–1184 (2019).

759 48. Kamravamanesh, D. *et al.* Increased poly-B-hydroxybutyrate production from
760 carbon dioxide in randomly mutated cells of cyanobacterial strain Synechocystis
761 sp. PCC 6714: Mutant generation and characterization. *Bioresour. Technol.* **266**,
762 34–44 (2018).

763 49. Henderson, R. A. & Jones, C. W. Physiology of poly-3-hydroxybutyrate (PHB)
764 production by Alcaligenes eutrophus growing in continuous culture.
765 *Microbiology* **143**, 2361–2371 (1997).

766 50. Thiel, K. *et al.* Redirecting photosynthetic electron flux in the cyanobacterium
767 Synechocystis sp. PCC 6803 by the deletion of flavodiiron protein Flv3. *Microb.*
768 *Cell Fact.* **18**, 1–16 (2019).

769 51. Tarawat, S., Incharoensakdi, A. & Monshupanee, T. Cyanobacterial production
770 of poly(3-hydroxybutyrate-co-3-hydroxyvalerate) from carbon dioxide or a single
771 organic substrate: improved polymer elongation with an extremely high 3-
772 hydroxyvalerate mole proportion. *J. Appl. Phycol.* **32**, 1095–1102 (2020).

773 52. Amerian Public Health Association. *Standard Methods for the Examination of*
774 *Water and Wastewater*. (2012).

775 53. Komárek, J., Kaštovský, J. & Jezberová, J. Phylogenetic and taxonomic
776 delimitation of the cyanobacterial genus aphanothece and description of anathece
777 gen. nov. *Eur. J. Phycol.* **46**, 315–326 (2011).

778 54. Komárek, J., Johansen, J. R., Šmarda, J. & Strunecký, O. Phylogeny and
779 taxonomy of synechococcus–like cyanobacteria. *Fottea* **20**, 171–191 (2020).

780 55. P, A. & J, T. Estimating cell numbers. in *Manual on Harmful Marine Microalgae*
781 (eds. G.M., H., D.M., A. & A.D., C.) 99–129 (UNESCO, 2004).

782 56. Bustin, S. A. A-Z of Quantitative PCR. in (ed. International University Line) 87–
783 112 (2004).

784 57. Lanham, A. B. *et al.* Determination of the extraction kinetics for the
785 quantification of polyhydroxyalkanoate monomers in mixed microbial systems.
786 *Process Biochem.* **48**, 1626–1634 (2013).

787 58. Tanweer, S. & Panda, B. Prospect of Synechocystis sp. PCC 6803 for synthesis
788 of poly(3-hydroxybutyrate-co-4-hydroxybutyrate). *Algal Res.* **50**, 101994 (2020).

789 59. Krasaesueb, N., Incharoensakdi, A. & Khetkorn, W. Utilization of shrimp
790 wastewater for poly-β-hydroxybutyrate production by Synechocystis sp. PCC
791 6803 strain ΔSphU cultivated in photobioreactor. *Biotechnol. Reports* **23**, e00345
792 (2019).

793 60. Krasaesueb, N., Promariya, A., Raksajit, W. & Khetkorn, W. Inactivation of
794 phosphate regulator (SphU) in cyanobacterium Synechocystis sp. 6803 directly
795 induced acetyl phosphate pathway leading to enhanced PHB level under
796 nitrogen-sufficient condition. *J. Appl. Phycol.* **33**, 2135–2144 (2021).

797 61. Carpine, R. *et al.* Genetic engineering of Synechocystis sp. PCC6803 for poly-β-
798 hydroxybutyrate overproduction. *Algal Res.* **25**, 117–127 (2017).

799

800 **Acknowledgements**

This research was supported by the European Union's Horizon 2020 research and innovation programme under the grant agreement No 101000733 (project PROMICON). B.A.A. thanks the Agency for Management of University and Research (AGAUR) for her grant [FIAGAUR_2021]. E.G.F. would like to thank the European Union-NextGenerationEU, Ministry of Universities and Recovery, Transformation and Resilience Plan for her research grant [2021UPF-MS-12]. J.G. acknowledges the support provided by the ICREA Academia program.

Author contributions

Conceptualization and experimental design by B.A.A., J.G. and E.G.F.; experimental work by B.A.A., A.L., A.L.M and M.A.; data analysis by B.A.A. and M.A.; writing – draft preparation by B.A.A. and M.A.; review and editing by J.G. and E.G.F.; project administration and funding acquisition by J.G. and E.G.F.

Competing interests

The authors declare no competing interests.

Materials & Correspondence

Correspondence and material requests should be addressed to Joan Garcia.

Tables Display items

Table 1. Average of the kinetic and stoichiometric parameters obtained during growth and accumulation phase of each cycle. Values presented in growth phase were measured when biomass reached stationary phase (see Fig. 1). Values in accumulation phase are the average value form both PBRs when the highest PHB content (%dcw) was obtained (at day 8 of accumulation phase in conditioning cycle; day 4 of accumulation phase in repetitions 1 and 2; and day 3 of accumulation phase in repetition 3).

	Growth phase			
	Conditioning	**Repetition**		
		1	**2**	**3**
VSS ($mg \cdot L^{-1}$)	802 ± 0.04	807 ± 0.09	818 ± 0.11	650 ± 0.05
μ (d^{-1})	0.52	0.17	0.18	0.16
$\Upsilon_{biomass}$ ($mgVSS \cdot L^{-1} \cdot d^{-1}$)	175.41	100	104.51	83.33
q_N($mgN \cdot gVSS \cdot d^{-1}$)	37.08	6.59	6.39	9.3
$Y_{X/N}$	14.03	16	16.72	10
Accumulation phase				

	Conditioning	Repetition		
		1	2	3
PHB (%dcw)	27 ± 2	27 ± 1	26± 3	28 ± 2
Υ_{PHB} (mgPHB·L^{-1}·d^{-1})	13.55 ± 0.24	15.79 ± 0.47	17.02 ± 0.65	19.74 ± 0.35
$Y_{PHB/Ac}$ (g PHBCOD/g AcCOD)	0.08 ± 0.02	1.14 ± 0.02	n.d.	n.d.

n.d. stands for no data.

Table 2. Comparison of PHB production with *Synechocystis* sp. PCC6803.

Genotype	Working volume (L)	Culture conditions	Accumulation time (days)	PHB fraction (%dcw)	Reference
WT	0.1	N-, P- & Ac+	21	33	[58]
WT (microbiome)	3	N-, P- & Ac+	14*	27	This study
WT	0.05	P- & Ac+	14	26	[9]
WT	0.05	N-, P- & Ac+	20	20	[36]
WT	0.15	N-, P- & Glc+	12	13	[8]
ΔPirC and OE PhaAB (*Cupriavidus necator*)	0.05	N-, P- & Ac+	20	81	[36]
ΔPirC and OE PhaAB (*Cupriavidus necator*)	0.05	N- & P-	20	63	[36]
OE PhaAB (native)	0.05	N- & Ac+	9	35	[10]
ΔSphU	15	Shrimp wastewater	11	33	[59]
ΔSphU	0.05	N+	14	15	[60]
OE Xfpk	0.08	N- & P-	30	12	[61]
OE PhaAB (*Cupriavidus necator*)	0.05	N- & Ac+	8	11	[18]

WT: wild-type; OE: overexpression; Δ: deletion; PirC: PII-interacting regulator; PhaA: beta-ketothiolase; PhaB: acetoacetyl-CoA reductase; SphU: phosphate regulator; Xfpk: phosphoketolase; N: Nitrogen; P: Phosphorus; Ac: Acetate; Glc: Glucose; -: defficiency; +: supplementation. *Note that all references are batch experiments, while in this study, three iterated accumulation phases have been performed with the same culture biomass, representing a total of 94 days of reactor operation.

Table 3. Culture conditions.

Period	Phase	IC (mg·L^{-1})	N (mg·L^{-1})	P (mg·L^{-1})	Ac (mg·L^{-1})	Lightness (h of light:dark)
Conditioning	Growth	100	50	0.1	-	15:09
	Starvation	-	-	-	600	0
Repetitions	Growth	-	25	0.1	-	15:09
	Starvation	-	-	-	600	0

834 **Figures**

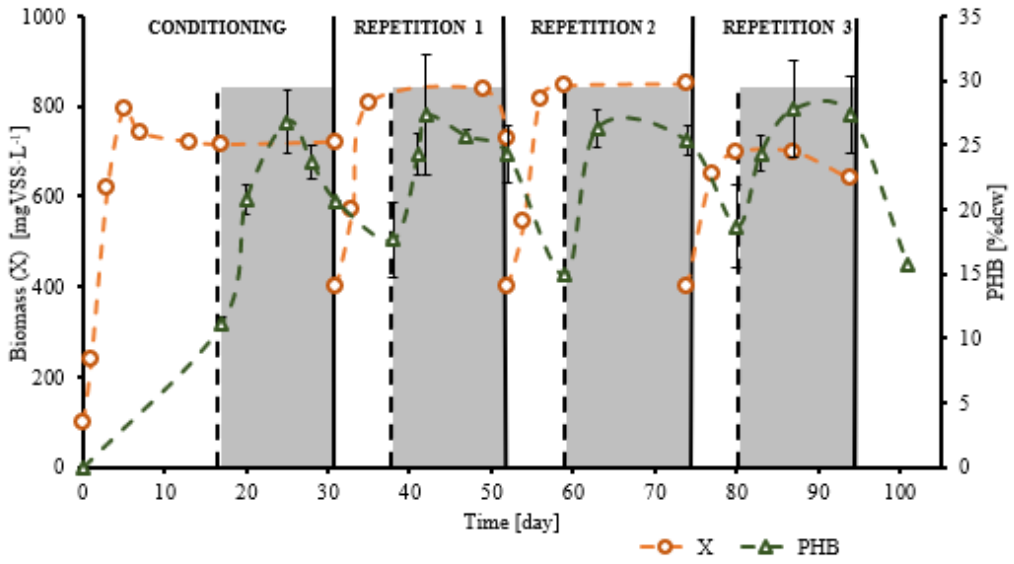

835

836 **Figure 1.** Average biomass (as VSS) and PHB evolution in PBR 1 & 2 of the microbiome
837 R3 for conditioning cycle and repetitions 1-3. Error bars indicate the standard deviation
838 of the replicates. Dashed vertical lines indicate the beginning of starvation phase and
839 vertical continuous black lines illustrate end of cycle (conditioning/repetition). Values of
840 biomass were estimated from turbidity measurements. PHB was not measured in growth
841 phase of each cycle.

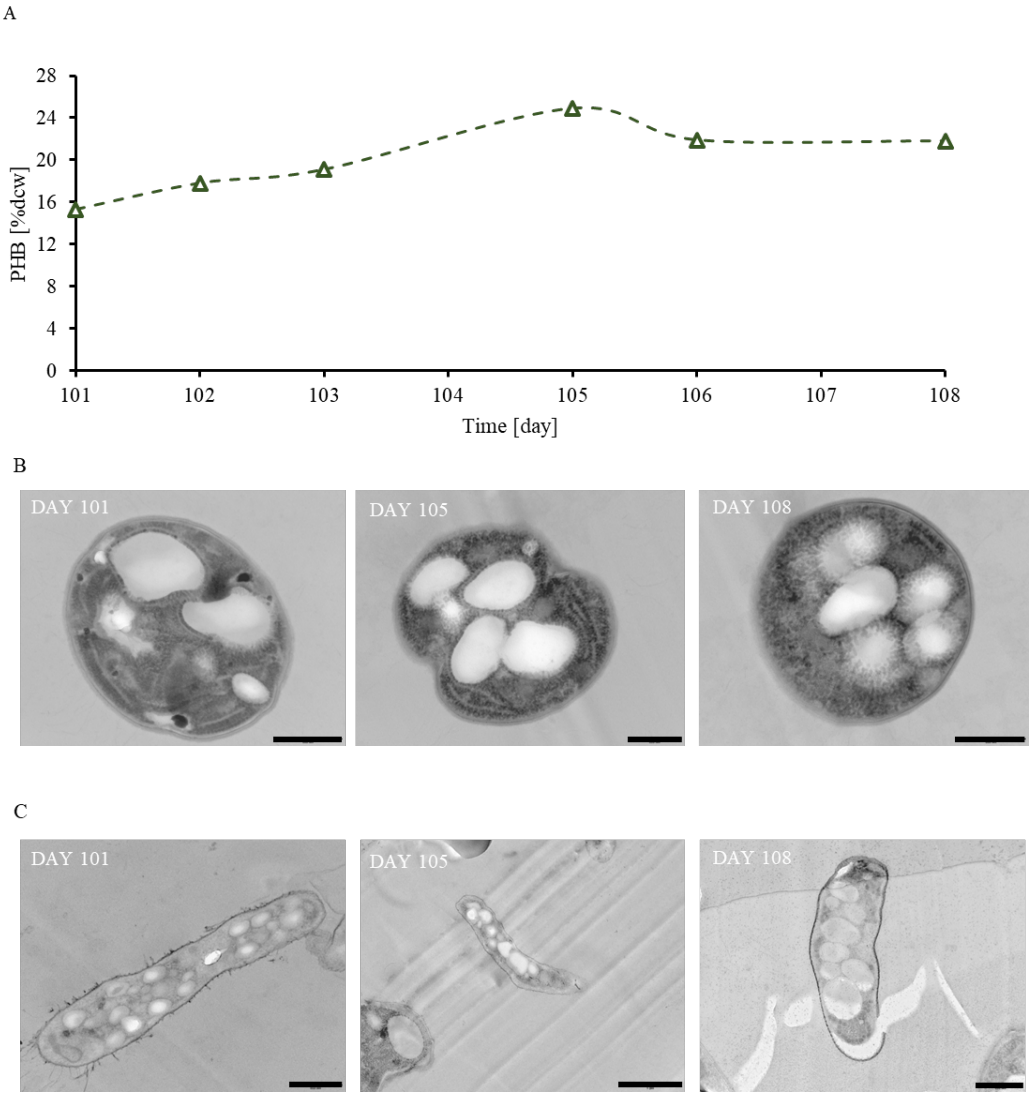

842

843 **Figure 2.** (A) Evolution of PHB production. TEM images of (B) *Synechocystis* sp. and
844 (C) *Synechoccocus* sp. from repetition 4. PHB granules are visible as white inclusions
845 inside the cell. Scale bar is 500 nm for all photos, except for photo (C) day 108, in which
846 scale bar is 1 µm.

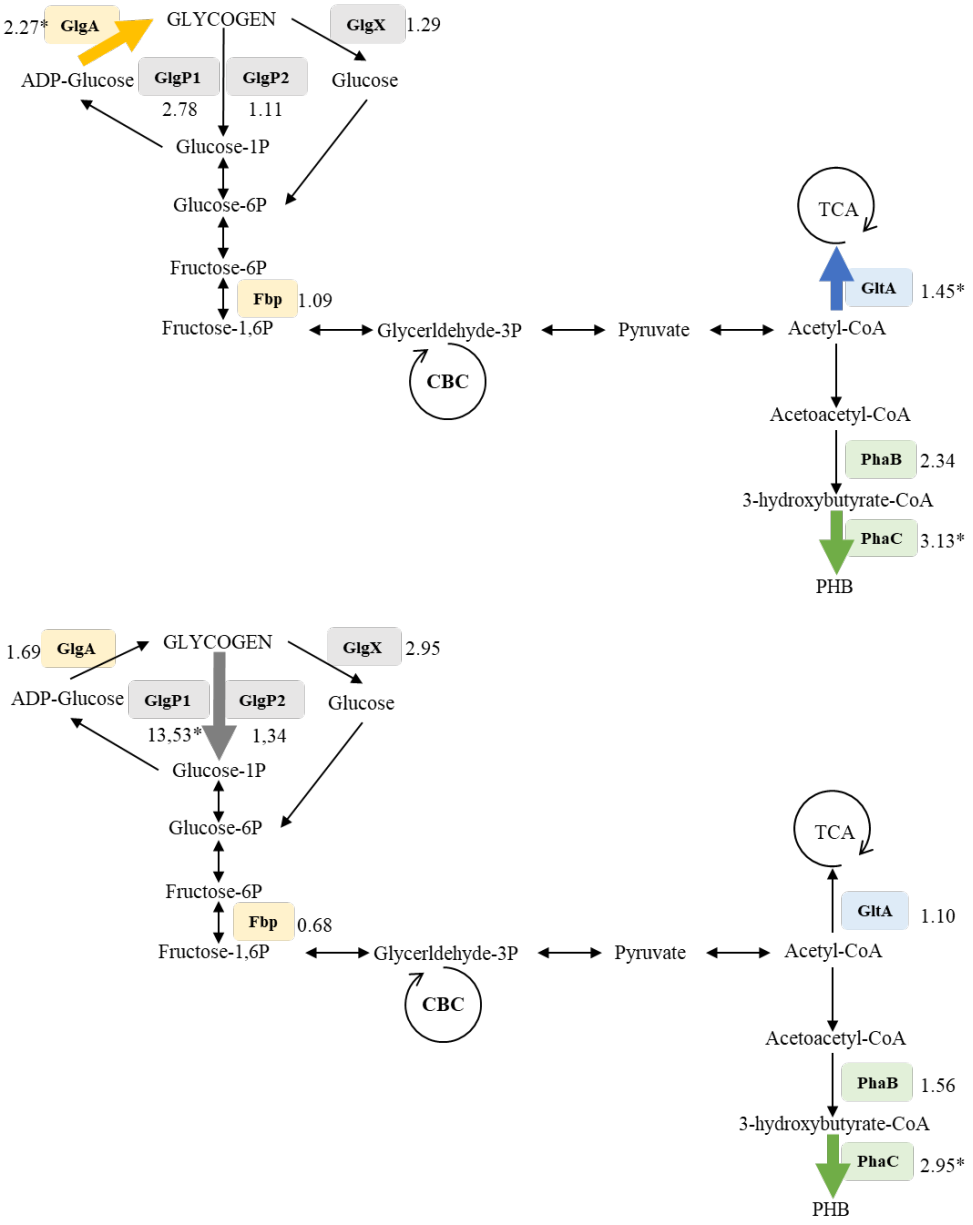

847

848 **Figure 3.** Schematic representation of biosynthetic pathways for PHB and glycogen
849 production in cyanobacteria. (A) corresponds to results from day 105 and (B) day 108.
850 Enzymes codified by the studied genes are shown in squares. Numbers next to enzymes
851 names represent the fold gene expression. * denotes genes with statistically significant
852 overexpression (p-value < 0.05). Yellow shows key enzymes involved in the synthesis of
853 glycogen (Fbp, GlgA); grey, to the glycogen catabolism (GlgP1, GlgP2, GlgX); green, to
854 the synthesis of PHB (PhaB, PhaC); and blue, to the introduction of acetyl-CoA into the
855 tricarboxylic acid (TCA) cycle (GltA). Abbreviations: Fbp: fructose-bisphosphatase 1
856 GlgA: glycogen synthase, GlgP1 and glgP2: glycogen phosphorylase, GlgX: glycogen

857 debranching enzyme, GltA: citrate synthase, PhaB: Acetyl-CoA reductase, PhaC: poly(3-
858 hydroxyalkanoate) synthase, TCA: tricarboxylic acid cycle, CBC: Calvin-Benson cycle.

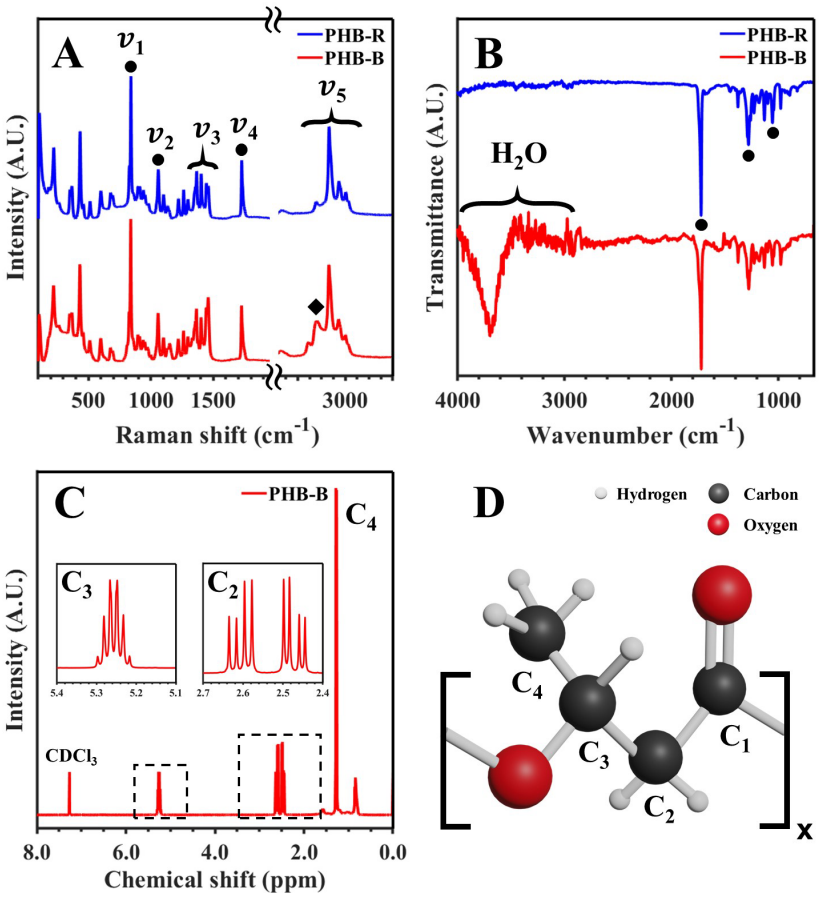

859

860 **Figure 4.** (A) Raman spectra for the PHB-R and PHB-B samples where the main Raman
861 active modes are marked with circles. The diamond highlights the shoulder attributed to
862 impurities during the extraction process. (B) FTIR spectra for the samples PHB-R and
863 PHB-B, where the region affected by the water and the vibrational modes (marked with
864 circles) can be observed. (C) ^{1}H-NMR spectra for the PHB-B sample with insets of the
865 relevant peaks and carbon assignation related to the monomer carbons. (D) Schematic
866 drawing of the PHB monomer with carbon numeration for NMR spectra interpretation.

867